

Article

Tailoring broadband inversion pulses for MAS Solid state NMR

Kerstin Riedel, Christian Herbst, Jörg Leppert, Oliver Ohlenschläger,
Matthias Görlach & Ramadurai Ramachandran*

Research group-Molecular Biophysics/NMR spectroscopy, Leibniz Institute for Age Research, Fritz Lipmann Institute, D-07745 Jena, Germany

Received 20 April 2006; Accepted 21 June 2006

Key words: double-quantum spectroscopy, inversion pulses, MAS, solid state NMR

Abstract

A simple approach is demonstrated for designing optimised broadband inversion pulses for MAS solid state NMR studies of biological systems. The method involves a two step numerical optimisation procedure and takes into account experimental requirements such as the pulse length, resonance offset range and extent of H_1 inhomogeneity compensation needed. A simulated annealing protocol is used initially to find appropriate values for the parameters that define the well known tanh/tan adiabatic pulse such that a satisfactory spin inversion is achieved with minimum RF field strength. This information is then used in the subsequent stage of refinement where the RF pulse characteristics are further tailored via a local optimisation procedure without imposing any restrictions on the amplitude and frequency modulation profiles. We demonstrate that this approach constitutes a generally applicable tool for obtaining pulses with good inversion characteristics. At moderate MAS frequencies the efficacy of the method is experimentally demonstrated for generating double-quantum NMR spectra via the zero-quantum dipolar recoupling scheme RFDR.

Introduction

A variety of dipolar recoupling techniques have been reported for inhibiting the spatial averaging of weak homo- and heteronuclear dipolar couplings under magic angle spinning conditions (Bennett et al., 1994; Griffin, 1998; Dusold and Sebald, 2000). Making use of these dipolar recoupling schemes, it is now possible in the solid state to achieve resonance assignments and to obtain structural constraints such as distances and torsion angles using isotopically labelled proteins and nucleic acids. This, in turn, has

facilitated MAS solid state NMR based structural studies of biological systems. Many of the commonly used dipolar recoupling sequences require the repeated application of rotor synchronised 180° pulses. For example, homonuclear dipolar recoupling via RFDR (Gullion et al., 1992; Bennett et al., 1992; 1998) typically involves the application of one inversion pulse per rotor period and heteronuclear dipolar recoupling via TEDOR (Hing et al., 1992) requires the application of either one or two dephasing inversion pulses per rotor period on the unobserved spins. Rotor synchronised application of RF pulses imposes restrictions on the maximum inversion pulse length that can be used in such experiments. Coupled with RF

*To whom correspondence should be addressed. E-mail: raman@fli-leibniz.de

pulse phase cycling generally implemented, the performance characteristics of the inversion pulses should be such that efficient dipolar recoupling over the required bandwidth can be achieved with sufficient tolerance to RF field inhomogeneities. Additionally, the RF field strength needed for dipolar recoupling should be as minimal as possible so as to avoid sample heating when RF irradiation is applied over extended periods of time and to reduce the interference between the decoupling and recoupling RF fields that could lead to signal loss (Bennett et al., 1998). A variety of difficulties impairing the efficacy of the recoupling sequence could arise when rectangular inversion pulses are used in dipolar recoupling schemes. For example, it may not be possible to minimise the interference between the recoupling and decoupling RF fields by simply reducing the recoupling RF field strength without also affecting the recoupling bandwidth. When broadband dipolar recoupling is required, the use of short high power rectangular inversion pulses can lead to poor recoupling efficiency, as in the case of RFDR. With recoupling schemes based on the CN_n^V and RN_n^V symmetry-based sequences (Carravetta et al., 2000; Brinkmann and Levitt, 2001; Levitt, 2002) using rectangular inversion pulses, the required RF field strength is related to the spinning speed employed. This can result in a situation where the RF field strength needed becomes either too large, that is beyond the hardware limits of the spectrometer system, or too small, leading to poor performance over a large bandwidth, and thereby affect the applicability of the sequence in certain spinning speed regimes.

To overcome some of these difficulties one can exploit the possibility to conveniently shape the RF pulse profile in the current generation of NMR spectrometers and make use of suitable amplitude and frequency/phase modulated inversion pulses instead of rectangular pulses. One such pulse that we have used extensively and effectively in several of our recent MAS solid state NMR studies (Leppert et al., 2002; Heise et al., 2002; Leppert et al., 2003; 2004a; Riedel et al., 2004a; Riedel et al., 2004b; Riedel, 2004c; Riedel et al., 2005) is the tanh/tan adiabatic inversion pulse constructed from the following adiabatic half passage and its time reversed half passage,

$$\omega_1(t) = \omega_{1(\max)} \tanh(\xi 2t/T_p)$$

$$\Delta\omega(t) = \Delta\omega_{\max} [\tan(\kappa(1 - 2t/T_p))] / \tan\kappa,$$

with $\xi = 10$, $\tan\kappa = 20$, $0 \leq t \leq T_p/2$, as originally reported (Hwang et al., 1998), and with R (representing the product of the pulsewidth and $\Delta\omega_{\max}$) value of 60. Among the different modulation functions proposed for generating adiabatic pulses, the tanh/tan amplitude and frequency modulation profiles have been found to be very time efficient for generating inversion pulses of short durations. The performance characteristics of RFDR and TEDOR with tanh/tan pulses were found to be superior to that seen with conventional rectangular pulses (Leppert et al., 2003; Riedel et al., 2005). However, it was observed that the RF power requirements for obtaining satisfactory response could also become substantially larger than what may be really necessary for the recoupling bandwidth needed, especially at high spinning speeds. In this context, it has been recently shown (Herbst, 2006a, b) that it is possible to minimise the RF field strength requirements by using optimal values for the R , $\tan\kappa$ and ξ parameters mentioned above (Tesiram et al., 2002). Taking into consideration the experimental constraints such as the maximum pulse length that can be used and inversion bandwidth required, the optimal parameter values were estimated via a simulated annealing (SA) protocol (Kirkpatrick et al., 1983; Herbst, 2006a, b). In this approach the tanh/tan inversion pulse was typically divided into $N=100$ intervals of equal duration with each element characterised by an amplitude and a phase value $\{a(t), \phi(t)\}_{i=1\dots N}$. Considering spin 1/2 nuclei, the net propagator, U_{net} , corresponding to the inversion pulse was first calculated for a chosen $\omega_{1(\max)}$. The density matrix $\rho(t)$ following this pulse was then obtained, starting from an initial state $\rho(0)$ of I_z . Optimal values for R , $\tan\kappa$ and ξ were obtained, for the chosen $\omega_{1(\max)}$, by minimising the error function $\varepsilon(\xi, \kappa, \Delta\omega_{\max})$, representing the deviation of the density matrix $\rho(t)$ from the required $\rho(\text{ideal})$, over a 2D grid of resonance offsets and RF field strengths. Where it was not possible for the chosen $\omega_{1(\max)}$ to obtain optimal values for R , $\tan\kappa$ and ξ that would lead to a satisfactory inversion profile, the SA procedure was repeated again using a different value for

$\omega_{1(\max)}$ until the best inversion profile was obtained with minimum RF field strength. The method outlined above has been demonstrated to perform satisfactorily. However, one of the difficulties with this approach is that generating optimised inversion pulses may be time consuming, with each SA run requiring a few hours for completion depending on the optimisation parameters. Additionally, the optimal parameter values obtained for a particular pulse width and inversion bandwidth may not represent the best values for a different pulse width and/or inversion bandwidth. Hence, for different experimental requirements, the corresponding minimum RF field strength and optimal parameter values have to be estimated individually.

Here we present an approach for speeding up the design of optimised broadband inversion pulses. The method makes use of the results from a SA optimisation calculation for further refinement via a local optimisation procedure, where the RF pulse characteristics are further tailored without imposing any restrictions on the amplitude and frequency modulation profiles. Inversion pulses generated via this approach were successfully employed for generating double-quantum ^{13}C NMR spectra of the ^{13}C -U specifically labelled triplet repeat expansion RNA (CUG) $_{97}$ (Leppert et al., 2004b).

Numerical and experimental procedures

For a tanh/tan pulse of a chosen duration, the optimal values of ξ , κ , and $\Delta\omega_{\max}$ that would lead

to satisfactory inversion performance over the desired range of resonance offsets are first estimated via the SA global optimisation approach using the minimum value possible for $\omega_{1(\max)}$. These calculations were carried out considering $\pm 10\%$ variations in the RF field strength, unless mentioned otherwise. The optimal parameter values obtained from SA get reflected in the N characteristic amplitude and phase values $\{a(t), \phi(t)\}_{i=1\dots N}$ that define the pulse shape. For generating 180° pulses with desired durations and inversion bandwidths, these $\{a(t), \phi(t)\}_{i=1\dots N}$ obtained from SA are used as starting input values to a local optimisation procedure. The downhill simplex method of Nelder and Mead (Press et al., 1992) was employed for local optimisation and the amplitude and frequency/phase modulation profiles of the pulse are allowed to vary freely so that a pulse with improved inversion characteristics can be obtained. As the efficacy of the local optimisation procedure is largely dependent on the initial simplex constructed, calculations were carried out with different starting simplexes to generate a suitable 180° pulse. Local optimisation calculations were carried out without any consideration to H_1 inhomogeneities. However, experimental studies with optimised inversion pulses in general reveal that the $m4$ phase cycling (Levitt et al., 1983) of the inversion pulses provides tolerance to $\sim \pm 10\%$ variation in the applied RF field strength (see below).

The inversion pulses reported in this study were employed for generating double-quantum NMR spectra at moderate magic angle spinning

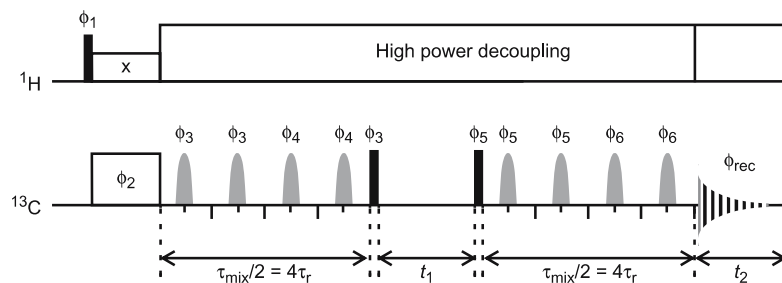


Figure 1. CPMAS RF pulse sequence employed for generating ^{13}C dipolar DQ NMR spectra. Filled rectangles represent 90° pulses. RFDR with inversion pulses applied at the centre of each rotor period was employed for ZQ dipolar recoupling during the mixing periods. The overall phasing scheme employed was (A): $\phi_1 = (y, -y)$; $\phi_2 = (2(y), 2(-x), 2(-y), 2(x))$; $\phi_3 = (2(x), 2(y), 2(-x), 2(-y))$; $\phi_4 = (2(-x), 2(-y), 2(x), 2(y))$; $\phi_5 = (8(x), 8(y), 8(-x), 8(-y))$; $\phi_6 = (8(-x), 8(-y), 8(x), 8(y))$; $\phi_{\text{rec}} = (2(y, -y, -y, y), 2(x, -x, -x, x), 2(-y, y, y, -y), 2(-x, x, x, -x))$. Phase sensitive 2D spectra were obtained by incrementing the phases ϕ_2 , ϕ_3 and ϕ_4 by 45° (States et al., 1982) with the spectral width in the ω_1 dimension set equal to the spinning speed employed.

frequencies via the RF pulse scheme given in Figure 1. This pulse sequence makes use of the RFDR approach and involves the application of rotor synchronised inversion pulses, one pulse per rotor period, for creating zero-quantum dipolar Hamiltonian of the form $\{I_1^- I_2^+ + I_1^+ I_2^-\}$ (Blanco et al., 2001; Riedel et al., 2006). Evolution of transverse magnetisation components, e.g. I_{1y} , under this ZQ Hamiltonian leads to the creation of anti-phase coherences, e.g. $I_{1x} I_{2z}$, and these are converted into DQ coherences by the application of a $\pi/2$ pulse. Similarly, anti-phase coherences, e.g. $I_{1x} I_{2z}$, created by the application of a $\pi/2$ pulse on a DQ coherence is converted back into an

observable single quantum coherence, e.g. I_{1y} , by the ZQ Hamiltonian. Standard phase cycling procedures were employed to select the desired coherence transfer pathway and phase sensitive 2D double-quantum spectra were generated via the SHR method (States et al., 1982) with ω_1 spectral width set to match the spinning speed employed. Experiments were carried out with an undiluted ^{13}C -U specifically labelled sample of (CUG) $_{97}$ at the spinning speeds indicated and at $\sim -10^\circ\text{C}$ on a 500 MHz wide-bore Varian ^{UNITY} INOVA solid state NMR spectrometer equipped with a 3.2 mm Chemagnetics triple resonance probe and waveform generators for pulse shaping. The RNA

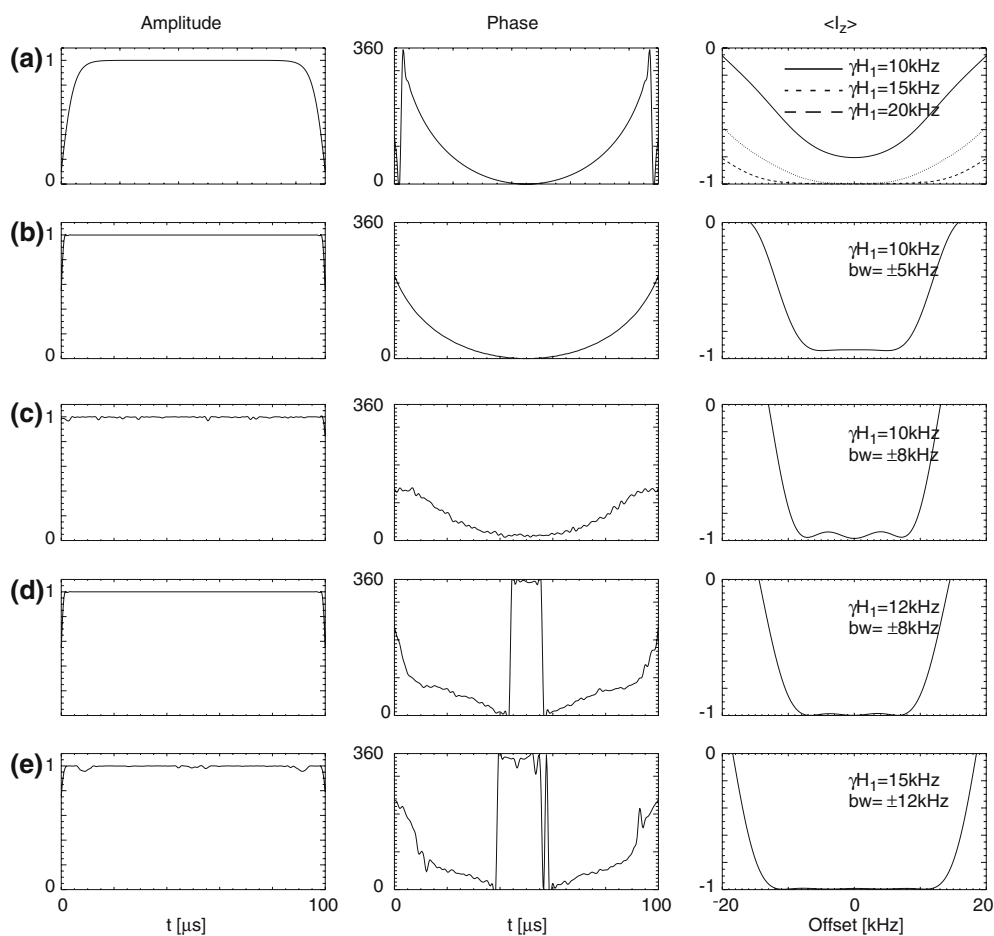


Figure 2. The amplitude, phase and inversion profiles of tanh/tan adiabatic pulse with R , $\tan \kappa$ and ζ values of 60, 20 and 10, respectively (a) and different optimised 180° pulses of $100\mu\text{s}$ duration (b–e). The RF field strength and inversion bandwidths for which the optimised inversion pulses were designed are also indicated. The performance at different applied RF field strengths are indicated for the tanh/tan pulse. Figure b shows the profiles for the tanh/tan pulse obtained via SA and having R , $\tan \kappa$ and ζ values of 10.5, 4.8 and 61.6, respectively. Figures c–e show the profiles for the pulses obtained via local optimisation using the amplitude and phase parameters of the pulse generated via SA.

sample was prepared using appropriately labelled rNTPs as described earlier (Leppert et al., 2004b). The frequency sweep is implemented in the spectrometer hardware as a phase modulation, $\phi(t) = \int \Delta\omega(t)dt$. Cross-polarisation under Hartmann–Hahn matching conditions was used and all spectra were collected under high power ^1H decoupling. The inversion pulses were phase-cycled according to the $m4$ phasing scheme.

Results and discussion

The amplitude, phase and inversion profiles of different 180° pulses considered/constructed in this study are given in Figures 2–4. Figure 2a shows the profiles for a tanh/tan pulse of $100\mu\text{s}$ duration

with R , tank and ξ values of 60, 20 and 10, respectively, as used in many of our recent studies. Figure 2b shows the profiles for an SA optimised inversion pulse with the same duration that was generated considering an inversion bandwidth of ± 5 kHz and $\omega_{1(\text{max})}$ of 10 kHz. The amplitude and phase parameters of this pulse were employed as starting input values for generating different inversion pulses via local optimisation. The profiles of these pulses and other relevant parameters are given in Figures 2c–e and 3a–e. The good inversion characteristics of the pulses generated clearly demonstrate the efficacy of the local optimisation approach, with each local optimisation computation taking only a few minutes for completion. For the inversion pulse widths and bandwidths considered in Figure 3a–e, we have also

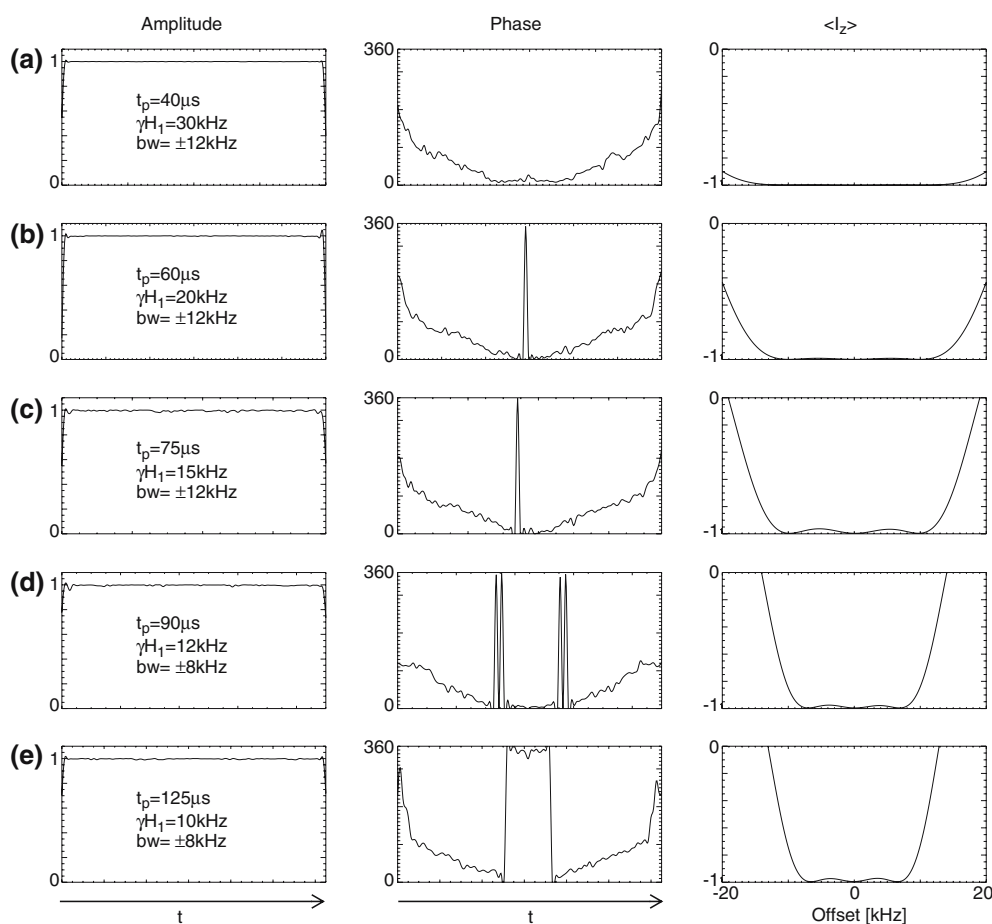


Figure 3. The amplitude, phase and inversion profiles of 180° pulses generated via local optimisation. The duration, RF field strength and inversion bandwidths for which the optimised inversion pulses were designed are indicated. All the pulses were obtained using the amplitude and phase parameters of the pulse generated via SA and shown in Figure 2b.

carried out local optimisation calculations employing other starting values. For example, with inversion pulses of 40, 60, 75, 90 and 125 μ s durations SA calculations were first carried out considering RF field strength and inversion bandwidths of (30 kHz, ± 20 kHz), (20 kHz, ± 10 kHz), (15 kHz, ± 10 kHz), (10 kHz, ± 8 kHz) and (10 kHz, ± 8 kHz), respectively. The optimised R , tank and ξ parameter values obtained for the above mentioned pulses were, respectively: (11.3, 4.4, 12.7), (13.2, 6.4, 46.8), (10.2, 4.3, 30.2), (10.4, 4.3, 92.8) and (73.1, 21.8, 99.7). Employing these optimised parameter values, local optimisation calculations were then carried out for the respective pulses considering

RF field strength and inversion bandwidths as in Figure 3. The amplitude, phase and inversion profiles of the pulses generated via this approach are given in Figure 4a–e. A comparison of the data presented in Figures 3 and 4 reveals that optimised pulses generated using different starting inputs to the local optimisation differ only marginally in the amplitude and phase profiles and the performance characteristics were invariably seen to be very similar. Hence, it is possible to use different inputs to the local optimisation procedure to derive inversion pulses with desired performance characteristics. We have employed in our SA calculation the tanh/tan profile for deriving the starting input amplitude and phase parameter values

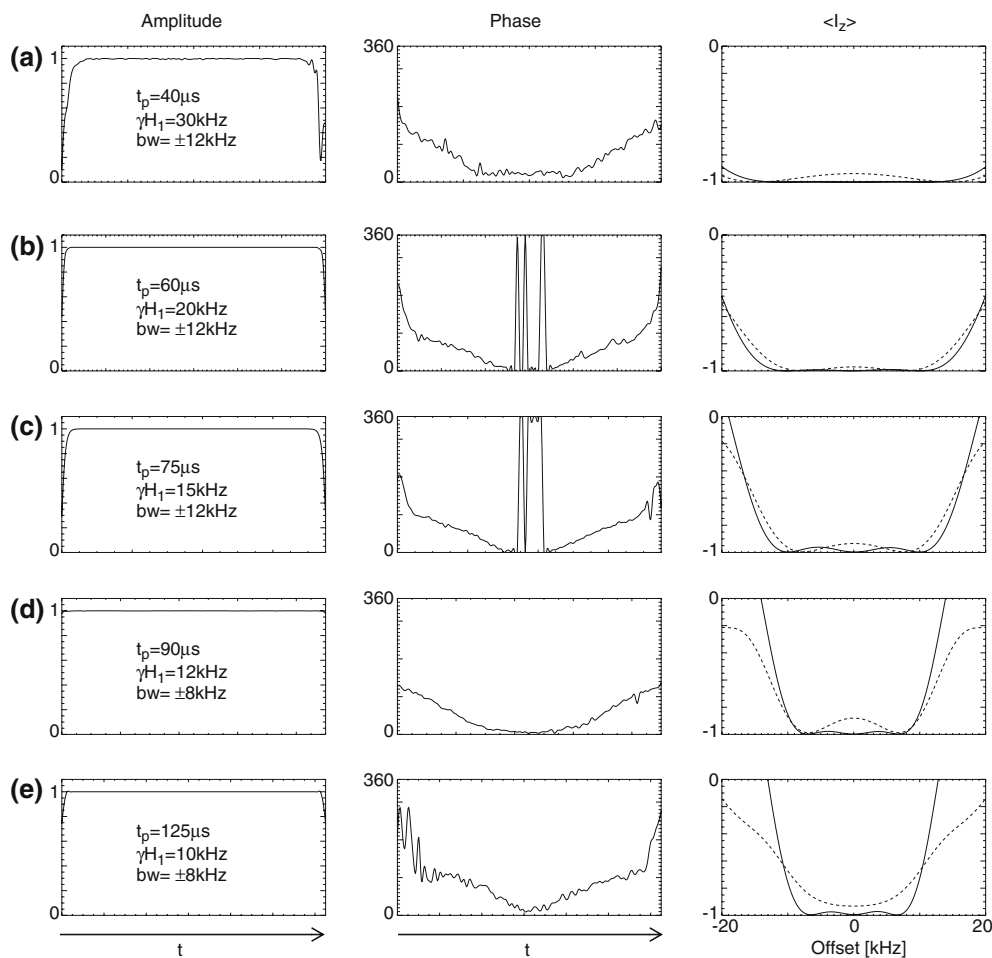


Figure 4. The amplitude, phase and inversion profiles of 180° pulses generated via local optimisation. The duration, RF field strength and inversion bandwidths for which the optimised inversion pulses were designed are indicated. These pulses were obtained using the amplitude and phase parameters of different inversion pulses generated via SA (see text for details). The inversion profiles of the 180° pulses generated via local optimisation and that derived via SA are indicated by the continuous and dashed lines, respectively.

needed for the local optimisation calculation. However, it is conceivable that in situations where long inversion pulses are required other pulse profiles could also be effectively used.

The inversion pulses reported in this work were constructed for exploring the possibilities for the efficient generation of ^{13}C DQ spectra of the sugar region of RNAs, at moderate magic angle spinning frequencies and via the pulse sequence given in Figure 1. DQ experiments are often used (Dam et al., 2002) for obtaining conformational constraints in biomolecular systems, e.g. sugar pucker in RNAs. With many of the inversion pulses designed in this work, the performance of the pulse sequence given in Figure 1 was evaluated via numerical simulations using the SIMPSON program (Bak et al., 2000) and it is seen that it is possible to effectively use these optimised pulses for obtaining DQ spectra (data not shown). Figure 5 shows the ^{13}C signals obtained for $t_1 = 0$ as a function of the ^{13}C recoupling RF field strength for different spinning speeds. The $m4$ phasing scheme applied for the optimised inversion pulses is found to provide sufficient tolerance to small variations in the ^{13}C RF field strength used. Figure 6 shows the double-quantum NMR spectra of the sugar region of the RNA, generated at the different spinning speeds indicated and with optimised inversion pulses. To avoid relayed magnetisation transfers, only short mixing times

corresponding to four rotor periods were employed when collecting these data. Experimental details are given in the figure caption. All the spectra show the expected strong peaks arising from short range (one-bond) homonuclear dipolar interactions. Experiments in which homonuclear ^{13}C DQ coherences evolve under the influence of the heteronuclear dipolar couplings involving protons attached to the sugar carbons are presently underway to obtain information about sugar ring conformations in $(\text{CUG})_{97}$. Although the inversion pulses were designed in the context of MAS solid state NMR studies, the method outlined here can be also extended to liquid state NMR investigations, e.g. for implementing efficient TOCSY sequences. Such studies are currently being pursued.

It is worth mentioning that other equally effective approaches, such as the method based on optimal control theory (Kobzar et al., 2004), have also been recently reported for the design of broadband inversion pulses. A detailed comparative study of the relative merits of the different procedures, however, is beyond the scope of the present study. The procedure outlined here is used routinely in our laboratory and is a robust approach that is easy to implement for generating inversion pulses according to the experimental requirements. In situations where very high spinning speeds are needed, e.g. to minimise the effects

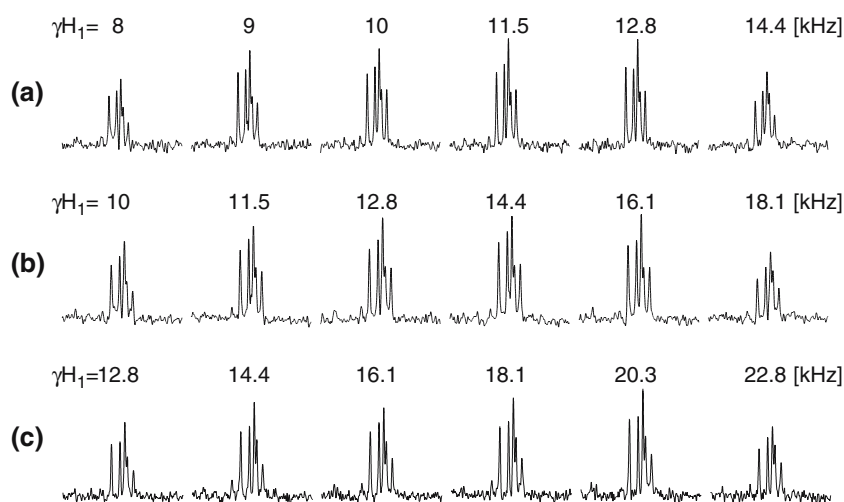


Figure 5. The experimental ^{13}C RNA signal intensities obtained ($t_1 = 0$) with the pulse sequence given in Figure 1 and as a function of the recoupling RF field strengths indicated. These data were generated at spinning speeds of 10,000 Hz (a), 12,000 Hz (b) and 14,000 Hz (c) using inversion pulses of 90, 75 and 60 μs durations as given in Figure 4.

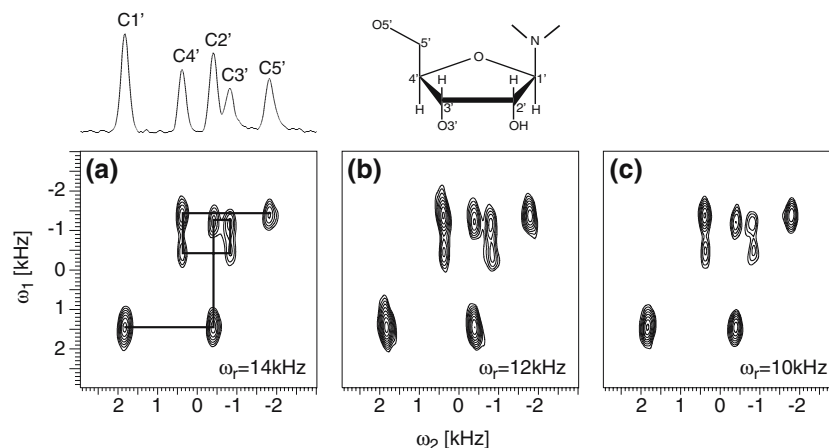


Figure 6. ^{13}C DQ NMR spectra of the sugar region of the $(\text{CUG})_{97}$ RNA collected at spinning speeds of 14,000 Hz (a), 12,000 Hz (b) and 10,000 Hz (c). Optimised inversion pulses of 60, 75 and 90 μs durations, as in Figure 4, were employed in obtaining these spectra using ^{13}C dipolar recoupling RF field strengths of ~ 18 , 14.5 and 11.5 kHz, respectively. Typically, 256 scans per t_1 increment, 1 s recycle time, 10 ms signal acquisition time were employed. Spin system connectivities, assignments of the resonances and the sugar moiety are also indicated.

of CSAs on the observed signal intensity, inversion pulses of short durations, e.g. in the range of 25–40 μs may be required. The present study shows also the possibilities for the design of such short broadband inversion pulses. Unlike other schemes used for the generation of DQ coherences (Karls-son et al., 2003), the RFDR approach permits the convenient optimisation of the RF power employed. It is not necessary to use high RF field strength if the required recoupling bandwidth is not very high, as in the present study of $(\text{CUG})_{97}$ RNA. It should also be possible to extend the approach outlined here for the design of band selective pulses and universal rotors. Such studies are planned. In conclusion the present study shows that by making use of the amplitude and phase parameters of any reasonably satisfactory tanh/tan inversion pulse it is possible to generate tailor made inversion pulses via local optimisation procedures and such pulses can be effectively used in MAS solid state NMR investigations.

Acknowledgements

This study has been funded in part by a PhD fellowship to Kerstin Riedel from Stiftung Stipendien-Fonds des Verbandes der Chemischen Industrie e.V. and a grant from the Deutsche Forschungsgemeinschaft (GO474/6-1). The Fritz-Lipmann-Institute (FLI) is a member of the Science

Association ‘‘Gottfried Wilhelm Leibniz’’ (WGL) and is financially supported by the Federal Government of Germany and the State of Thuringia.

References

- Bak, M., Rasmussen, J.T. and Nielsen, N.C. (2000) *J. Magn. Reson.*, **147**, 296–330.
- Bennett, A.E., Ok, J.H., Griffin, R.G. and Vega, S. (1992) *J. Chem. Phys.*, **96**, 8624–8627.
- Bennett, A.E., Griffin, R.G., Vega, S. (1994) *NMR Basic Principles and Progress*, Vol. 33, Springer Verlag, Berlin, 1–77.
- Bennett, A.E., Rienstra, C.M., Griffiths, J.M., Zhen, W., Lansbury, P.T. and Griffin, R.G. (1998) *J. Chem. Phys.*, **108**, 9463–9479.
- Blanco, F.J. and Tycko, R. (2001) *J. Magn. Reson.*, **149**, 131–138.
- Brinkmann, A. and Levitt, M.H. (2001) *J. Chem. Phys.*, **115**, 357–384.
- Carravetta, M., Eden, M., Zhao, X., Brinkmann, A. and Levitt, M.H. (2000) *Chem. Phys. Lett.*, **321**, 205–215.
- Dam, L.V., Ouwerkerk, N., Brinkmann, A., Raap, J. and Levitt, M.H. (2002) *Biophys. J.*, **83**, 2835–2844.
- Dusold, S. and Sebald, A. (2000) *Annu. Rep. NMR Spectrosc.*, **41**, 185–264.
- Griffin, R.G. (1998) *Nature Struct. Biol.*, **5**, 508–512.
- Gullion, T. and Vega, S. (1992) *Chem. Phys. Lett.*, **194**, 423–428.
- Heise, B., Leppert, J., Ohlenschläger, O., Görlach, M. and Ramachandran, R. (2002) *J. Biomol. NMR*, **24**, 237–243.
- Herbst, C. (2006a) Diploma Thesis, Friedrich-Schiller-University, Jena.
- Herbst, C., Riedel, K., Leppert, J., Ohlenschläger, O., Görlach, M., Ramachandran, R. (2006b) *J. Biomol. NMR*, (in press).
- Hing, A.W., Vega, S. and Schaefer, J. (1992) *J. Magn. Reson.*, **96**, 205–209.

- Hwang, T., van Zijl, P.C.M. and Garwood, M. (1998) *J. Magn. Reson.*, **133**, 200–203.
- Karlsson, T., Popham, J.M., Long, J.R., Oyler, N. and Drobny, G.P. (2003) *J. Am. Chem. Soc.*, **125**, 7394–7407.
- Kirkpatrick, S., Gelatt, C.D. and Vecchi, M.P. (1983) *Science*, **220**, 671–680.
- Kobzar, K., Skinner, T.E., Khaneja, N., Glaser, S.J. and Luy, B. (2004) *J. Magn. Reson.*, **170**, 236–243.
- Leppert, J., Heise, B., Görlach, M. and Ramachandran, R. (2002) *J. Biomol. NMR*, **23**, 227–238.
- Leppert, J., Heise, B., Ohlenschläger, O., Görlach, M. and Ramachandran, R. (2003) *J. Biomol. NMR*, **26**, 13–24.
- Leppert, J., Ohlenschläger, O., Görlach, M. and Ramachandran, R. (2004a) *J. Biomol. NMR*, **29**, 167–173.
- Leppert, J., Urbinati, C.R., Häfner, S., Ohlenschläger, O., Swanson, M.S., Görlach, M. and Ramachandran, R. (2004b) *Nucleic Acids Res.*, **3**, 1177–1183.
- Levitt, M.H. (2002) *Encyclopedia NMR*, **9**, 165–196.
- Levitt, M.H., Freeman, R. and Frenkiel, T. (1983) *Adv. Magn. Reson.*, **11**, 47–110.
- Press, W.H., Teukolsky, S.A., Vetterling, W.T. and Flannery, B.P. (1992) *Numerical Recipes in C*. Cambridge University Press, Cambridge, pp. 408–412.
- Riedel, K., Leppert, J., Ohlenschläger, O., Görlach, M. and Ramachandran, R. (2004a) *Chem. Phys. Lett.*, **395**, 356–361.
- Riedel, K., Leppert, J., Häfner, S., Ohlenschläger, O., Görlach, M. and Ramachandran, R. (2004b) *J. Biomol. NMR*, **30**, 389–395.
- Riedel, K. (2004c) Diploma thesis, Friedrich-Schiller-University, Jena.
- Riedel, K., Leppert, J., Ohlenschläger, O., Görlach, M. and Ramachandran, R. (2005) *J. Biomol. NMR*, **31**, 49–57.
- Riedel, K., Herbst, C., Leppert, J., Ohlenschläger, O., Görlach, M. and Ramachandran, R. (2006) *Chem. Phys. Lett.*, **424**, 178–183.
- States, D.J., Haberkorn, R.A. and Ruben, D.J. (1982) *J. Magn. Reson.*, **48**, 286–292.
- Tesiram, Y.A. and Robin Bendall, M. (2002) *J. Magn. Reson.*, **156**, 26–40.